Degradation of a textile dye, Rhodamine 6G (Rh6G), by heterogeneous sonophotoFenton process in the presence of Fe-containing TiO₂ catalysts

Nazlı Demir · Gönül Gündüz · Meral Dükkancı

Abstract In this study, degradation of Rhodamine 6G (Rh6G) was investigated with ultrasound-assisted heterogeneous photoFenton process by iron-containing TiO_2 catalysts. The catalysts were prepared by incipient wetness impregnation method and characterized by XRD, SEM, FT-IR, nitrogen adsorption, and ICP-AES measurements. Almost complete color removal (99.9 %) was achieved after a reaction time of 90 min while chemical oxygen demand (COD) could be removed by 24 % only with the 1 wt% iron-containing TiO_2 catalyst. Initial color removal after 15 min of reaction and total COD abatement after 90 min of reaction decreased with increasing calcination temperature of the catalyst from 573 to 973 K. This indicated that the catalytic activity of the catalyst depend on the percentage of anatase phase in the TiO_2, which was decreased with increasing calcination temperature.

Introduction

During the textile dyeing process, large amounts of wastewater are produced and discharged into the environment. These effluents usually contain toxic dyes which exhibit low biodegradability. The strong color of dyes makes them visible even at very low concentration, and this causes serious aesthetic and pollution problems in wastewater disposal. The strong absorption of sunlight by dyes reduces the photosynthetic

N. Demir · G. Gündüz (✉) · M. Dükkancı
Engineering Faculty, Chemical Engineering Department,
Ege University, 35100 Bornova, Izmir, Turkey
e-mail: gonul.gunduz@ege.edu.tr

activity of aquatic plants and threats seriously the whole ecosystem.

Conventional processes such as biological treatment, coagulation, and adsorption are ineffective for decolorization and degradation of dyes. Hence, studies on degradation of dyes have been centered on advanced oxidation processes which are characterized by the same chemical feature: production of OH˙ radicals. In this concern, catalytic methods provide complete degradation of dyes. Of particular interest, in this regard, is the oxidizing system based on the homogeneous Fenton reagent ($Fe^{2+}/Fe^{3+}/H_2O_2$). However, a number of disadvantages, such as impossible regeneration of the catalyst, narrow range of pH values at which the reaction occurs, and necessity of removal of iron compounds from purified water, restrict the possible application field of this system. These problems can be resolved by using heterogeneous catalysts in which iron is immobilized within the structure of a porous solid (Neamtu et al. 2008; Dutta et al. 2001; Torrades et al. 2004; Neamtu et al. 2003).

PhotoFenton oxidation is the photocatallically enhanced version of the Fenton process. UV light irradiation causes an increase in the OH˙ formation rate and efficiency via photo-reduction of Fe^{3+} to Fe^{2+}, thus further react with more H_2O_2 molecules as long as H_2O_2 is available. On the other hand, TiO_2 is a well-known photocatalyst and when TiO_2 is radiated with light energy greater than its band gap energy (3.2 eV), electrons and holes are generated. The holes react with OH^- or water to produce OH˙ radicals (heterogeneous photo catalysis). The recombination of electrons and holes, which is a drawback of photo catalytic efficiency, can be reduced by addition of transition metals such as iron as dopant and photocatalytic efficiency can be improved (Konstantinou and Albanis 2004; Jamalluddin and Abdullah 2011; Sun et al. 2012; Arana et al. 2002; Akpan and Hameed 2009; Feng et al. 2004; Liu et al. 2006; Souza et al. 2011; Buddee et al. 2011; Stasinakis 2008). Combination of heterogeneous

photocatalysis with heterogeneous Fenton reaction is considered to be cost-effective as long as this combination produces a synergetic effect (Bouras and Lianos 2008). If heterogeneous photoFenton oxidation technique is used in combination with the ultrasonic irradiation (sonolysis, which is another advanced oxidation technique), not only the rate of generation of OH• radicals will be increased but also mass transfer limitations affecting photoFenton technique will be avoided.

Also the turbulence created by ultrasonic irradiation helps in cleaning of the catalyst surface which increases its efficiency (Jiang et al. 2002; Sivakumar et al. 2002; Nam et al. 2003; Okuno et al. 2000). Little attention has been paid on coupling ultrasound with other advanced oxidation process. In recent years, the simultaneous use of ultrasound and photocatalysis, sonophotocatalysis, has been studied to degrade dyes (He et al. 2007; Ince and Tezcanlı 2001; Wang et al. 2003; Tezcanlı-Güyer and İnce 2003, 2004; Rehopek et al. 2004; Kusic et al. 2006; Berberidou et al. 2007; Zhong et al. 2011). So far, no study has been conducted regarding to use of an integrated heterogeneous sonophotoFenton process based on the use of Fe/TiO$_2$ catalysts for degradation of dyes.

In this study, Rh6G was selected as a model dye, because it has a high molar absorptivity and a high photostability. Hence, it is an ideal substance for an oxidation study including photo oxidation (Elfeky and Al-Sherbini 2011).

A few studies have been reported on the degradation of Rh6G by the simultaneous use of different advanced oxidation process. The studies have been mainly focused on degradation of Rh6G by photocatalytic oxidation in presence of TiO$_2$ (Chen et al. 2003; Kansal et al. 2007; Aarthi and Madras 2007; Beyers et al. 2009; De Witte et al. 2008; Meng et al. 2012; Asiri et al. 2011; Ghazzal et al. 2012) or by wet peroxide oxidation over iron or iron- and copper-containing zeolite catalysts (Dükkancı et al. 2010a, b; Prihodko et al. 2011). For the first time, in this study, an integrated heterogeneous sonophotoFenton process based on iron-containing TiO$_2$ catalyst prepared by incipient wetness impregnation method was used for degradation of Rhodamine 6G.

Experimental

Catalyst preparation

Iron-containing TiO$_2$ catalysts were prepared by incipient wetness impregnation method used by Arana et al. (2002). Aqueous solution of Fe(NO$_3$)$_3$.9H$_2$O (Sigma-Aldrich) was added slowly to proper amount of TiO$_2$ (Sigma-Aldrich P-25, 80 % anatase), and the mixture was stirred vigorously for 48 h. Then, the water of the mixture was evaporated by heating at 393 K for 24 h. The catalyst was calcined at 773 K for 3 h. The catalysts have been denoted as TiO$_2$ for bare TiO$_2$ Sigma-Aldrich P-25 and x Fe/TiO$_2$ for the doped catalysts,

where x is the Fe weight % (wt%) in the catalyst. x was changed to be 1 and 5. Catalyst containing 1 wt% iron was calcined at 573, 773, and 973 K in order to investigate the effect of calcination temperature on the catalytic activity in the degradation of Rh6G.

Catalyst characterization

Powder X-ray diffraction (XRD) patterns of the catalysts were recorded in the range of 5–80° by Philips X'Pert Pro with Cu-Kα radiation to determine in the crystalline structure of the samples. Morphological properties were analyzed by scanning electron microscopy (FEI Quanta250 FEG). Nitrogen adsorption and desorption isotherms at 77 K were measured using Micromeritics ASAP 2010 equipment. FT-IR spectra were recorded in the 650–3,650 cm^{-1} with a Perkin Elmer Spectrum 100 spectrometer. The contents of iron of the samples were determined by a Varian-96 inductively coupled plasma atomic emission spectrometer (ICP-AES).

Catalytic activity tests

Heterogeneous Fenton-like degradation of Rh6G

The heterogeneous Fenton-like degradation of Rhodamine 6G (Sigma Aldrich) was performed under isothermal conditions in a temperature-controlled shaded glass batch reactor equipped with a mechanical stirrer and a pH electrode. In a typical run, 150 cm^3 of aqueous dye solution of $4×10^{-5}$ M (0.02 g/dm^3) was placed into the reactor and the temperature was adjusted to 323 K. When the temperature reached to 323 K, pH of solution was measured and 0.15 g of catalyst (1 g/dm^3) was introduced into the solution under continuous stirring (350 rpm). After stabilization of the temperature at 323 K, pH of solution was again measured and the solution was analyzed in order to determine whether the dye is adsorbed by the catalyst. Then a solution of 70 mM of 35 % H$_2$O$_2$ (Merck) was added into the dye solution. A run took 2 h. The samples taken periodically were centrifuged for 30 min and then analyzed with UV spectrophotometer (Jasco 7800 UV-vis). The decrease of intensity of the band at 523 nm was used as a measure of decolorization degree. All the runs were carried out at the dye initial pH (pH 6.9). No attempt was made to change the solution pH during the runs.

In addition to these measurements, chemical oxygen demand (COD) removal of the dye solution was determined by measuring initial COD and final COD (at the end of the run) of dye solution with a COD device (Lovibond Checkit Direct COD Vario). Garden Cress (*Lepidium sativum* L.) was used to assess the acute ecotoxicity of Rh6G samples prior to and after treatment.

UV light assisted heterogeneous Fenton-like degradation of Rh6G

These experiments were carried out in the experimental set-up given in the "Heterogeneous Fenton-like degradation of Rh6G" section under the same reaction conditions with a UV-C lamp (Philips TUV, 8 W) located horizontally at the top of the glass reactor. The system was covered with an aluminum foil to prevent the reaction mixture from the sun light.

Degradation of Rh6G using sonophotoFenton process

Catalytic runs with the combination of ultrasound and UV with heterogeneous Fenton process were performed in order to determine benefits of combined techniques in the oxidation process.

A simplified scheme of the experimental set-up used for these runs is presented in Fig. 1.

In a typical experiment, 650 mL of 4×10^{-5} M (20 ppm) of Rh6G aqueous solution was poured into the cylindrical reactor and 0.5 g/dm^3 of catalyst was added into the solution and the suspension was left for 30 min in the dark to establish the adsorption-desorption equilibrium of the dye on catalyst surface. The amount of the dye adsorbed by the catalyst was determined by measuring the dye concentration after 30 min in the absence of UV illumination and ultrasound. Then 70 mM of H_2O_2 was added and the UV lamps and the sonicator were turned on. The solution was irradiated with two UV-C lamps (each 4 W). A titanium-made probe at a frequency of 20 kHz with a power output of 40 W (Bandelin Sonopuls, HD3200) immersed in the liquid was used to deliver the ultrasound energy in the reaction mixture. Heterogeneous sonophotoFenton process for degradation of dye took 90 min. The reaction temperature was kept constant at 293 ± 2 K by circulating cooling water (PolyScience, 9106) around the reactor to avoid significant overheating of the reaction media. The reaction vessel was maintained in a box to avoid photochemical reactions induced by natural light. Experiments were performed at Rh6G ambient pH which was 6.9 and left uncontrolled during the experiments. Samples of about 4 ml were periodically drawn from the vessel, and
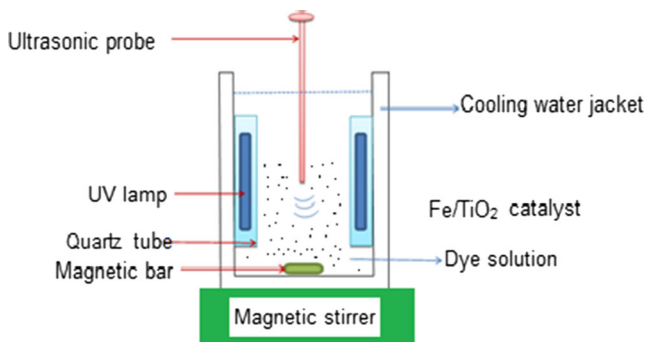

Fig. 1 SonophotoFenton oxidation set-up

reaction was stopped by keeping the samples in iced-water. After centrifugation, samples were subjected to analysis.

Results and discussion

X-ray diffraction studies

XRD patterns of TiO_2 samples prepared are displayed in Fig. 2.

The peaks at $2\theta = 25.4, 37.9, 48.1, 53.9, 55.2,$ and $62.9°$ are attributed to the diffractions of the anatase phase (Fig. 2a). After the incorporation of iron into the TiO_2, the peaks intensity weakened (Jamalluddin and Abdullah 2011; Zhao et al. 2011). The decrease in the peak intensities in the Fe/TiO_2 samples can be attributed to the enhanced absorption of X-ray due to iron cation (Dükkancı et al. 2010a). However, the peak intensity of anatase phase of TiO_2 at $2\theta = 25.4°$ for catalyst 5 % Fe/TiO_2 at 773 K is higher than that for 1 % Fe/TiO_2 at 773 K (see in Fig. 2a). The reason of this difference may be the existence of agglomerates in sample of 5 % Fe/TiO_2 rather than the individual particles (Hafizah and Sopyan, 2009, Jiefang et al. 2003). The peaks at $2\theta = 27.5, 36.0,$ and $41.2°$ are attributed to rutile phase (Khalid et al. 2013).

Figure 2b represents the XRD patterns of 1 % Fe/TiO_2 catalyst calcined at different temperatures ranging from 573 to 973 K. As the calcination temperature was raised to 973 K, peak intensity of rutile phase became stronger and anatase structure showed weaker intensities of the diffraction peaks. The phase percentage formed was determined from the integrated intensity at $2\theta = 25.4°$ for anatase and the peak at $2\theta = 27.5°$ for rutile. The percentages of anatase, (A (%)), was determined as follows:

$$A, (\%) = \frac{100}{1 + 1.265(I_R/I_A)} \tag{1}$$

where I_R = intensity of the rutile peak and I_A = intensity of the anatase peak. Crystallite sizes (C_s) of the catalysts were calculated from the half-height width of peaks of anatase and rutile using Scherrer equation (Tayade et al. 2007).

$$C_s = \frac{K\lambda}{\beta \cos\theta} \tag{2}$$

where β = line width at half maximum height, θ = diffraction angle, K = shape factor of 0.9, λ = the wave length of X-ray radiation (CuKα = 0.15405 nm).

The percentage of anatase phase and crystallite size of the samples are summarized in Table 1.

The incorporation of iron into the TiO_2 caused an increase in the crystallite sizes in anatase and rutile phases. At calcination temperature higher than 573 K, the crystallites formed were larger in size at both phases, which can be attributed to

Fig. 2 X-ray diffraction patterns of catalysts. **a** The catalysts prepared by incipient wetness impregnation method with different Fe loadings. **b** One percent Fe/TiO₂ catalysts calcined at 573, 773, and 973 K
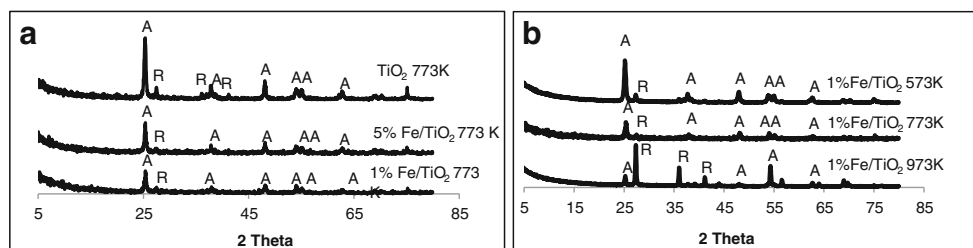
the thermally promoted crystallite growth (Khalid et al. 2013). The increase of calcination temperature from 573 to 973 K caused a decrease in the percentage of anatase phase from 81 to 15.9 % due to the occurrence of the anatase to rutile transformation. It was seen that the crystallite size in anatase phase decreased slightly with the increase of iron content from 1 to 5 wt% for the samples calcined at 773 K. Similar results have been reported in literature for the crystallite sizes and the percentage of anatase phase in the iron-containing TiO₂ catalyst (Jamalluddin and Abdullah 2011; Sun et al. 2012; Zhao et al. 2011; Khalid et al. 2013; Tayade et al. 2007; Hafizah and Sopyan 2009; Mi et al. 2013). The crystal size calculated for rutile phase of 5 % Fe/TiO₂ catalyst at 773 K was quite big (121.1 nm). It may be attributed to the broadening and low density in diffraction peak of rutile phase of TiO₂ at $2\theta = 27.5°$, which makes difficult the application of Eq. 2 to the sample (Khalid et al. 2013).

FT-IR measurements

FT-IR spectra of the catalyst samples are depicted in Fig. 3 in the range of $650-3{,}650$ cm⁻¹.

The broad band at the range of $3{,}150-3{,}650$ cm⁻¹ observed is assigned to the Ti–OH stretching band (Tayade et al. 2007). As the calcination temperature was raised from 773 to 973 K, the broad band between 3,150 and 3,650 cm⁻¹ disappear, which is an evidence of anatase to rutile transformation (Khalid et al. 2013), while no significant change is observed at the same band with the increase of calcination temperature from 573 to 773 K. The intensity of this broad band decreases

with increasing amount of iron added to TiO₂ sample (Fig. 3a). The band at 1,640 cm⁻¹ indicates the deformation vibration, which is evidence for the large amount of water molecules. The complete removal of the absorption band at 1,640 cm⁻¹ for the sample calcined at 973 K shows the absence of hydroxyl groups in this rutile-formed TiO₂.

SEM studies

Figure 4 displays the morphology of the samples. The surface of TiO₂ sample without iron looked coral-like and heavily aggregated particles of very small crystallites were observed. Insertion of low amount of iron (1 %) into the TiO₂ did not change significantly the SEM image of TiO₂. However, insertion of high amount of iron (5 %) into the TiO₂ separated the aggregates of TiO₂ particles from each other, which caused a slight decrease in pore volume and surface area of the sample (Zhao et al. 2011; Khalid et al. 2013; Hossenia et al. 2010).

ICP analysis

The content of iron in the samples was determined by ICP-AES analysis. Table 2 presents these results. As seen, the calculated iron contents are very close to the measured ones by ICP.

Nitrogen adsorption measurements

The BET-surface area (S_{BET}), total pore volume (V_p), and mean pore diameter (d_{mean}) obtained from nitrogen adsorption/desorption measurements are presented in Table 2. Figure 5 displays the nitrogen adsorption studies of prepared catalysts.

With increasing the calcination temperature, the mean pore diameter and total pore volume of samples decrease. A slight decrease in the surface area is observed with increasing the doping level of Fe at a calcination temperature of 773 K, while a sharp reduction (three times) in the surface area was obtained when 1 % Fe/TiO₂ catalyst was calcined at 973 K. These results are in agreement with ones for Fe/TiO₂ catalysts prepared by incipient wetness impregnation method published by Arana et al. (2002, 2003) and by Akpan and Hameed (2009). As seen from Fig. 5, nitrogen adsorption isotherms of the samples are of type II according to

Table 1 Crystallite sizes and the percentage of anatase phase of the catalysts prepared

Catalysts	Crystallite size, nm		Anatase, %
	Anatase	Rutile	
TiO₂, 773 K	20.7	36.9	79.8
1 % Fe/TiO₂, 573 K	20.9	27.3	81.0
1 % Fe/TiO₂, 773 K	24.0	65.4	73.3
1 % Fe/TiO₂, 973 K	40.7	31.4	15.9
5 % Fe/TiO₂, 773 K	22.6	121.1	80.3

Fig. 3 FTIR spectra of catalysts. **a** The catalysts prepared by incipient wetness impregnation method with different Fe loadings. **b** One percent Fe/TiO$_2$ catalysts calcined at 573, 773, and 973 K
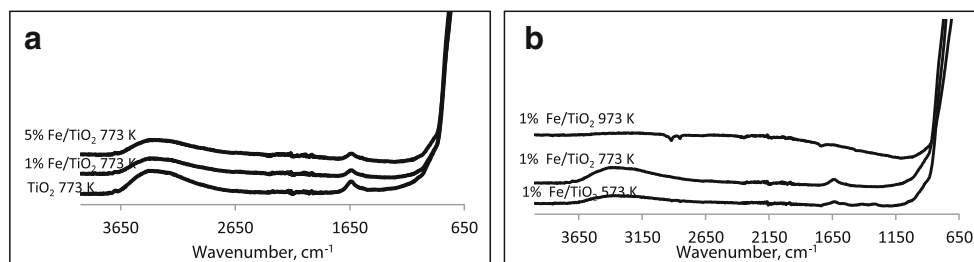
IUPAC classification which is a similar result with the study done by Wang et al. (2004).

Catalytic activity tests

Catalytic activity tests were repeated at least two times, mostly three times.

Fig. 4 SEM images of catalysts. **a** One percent Fe/TiO$_2$, 773 K, **b** 5 % Fe/TiO$_2$, 773 K, and **c** TiO$_2$, 773 K

Heterogeneous Fenton-like degradation of Rh6G

Figure 6 presents the results on heterogeneous Fenton-like degradation of Rh6G with iron free TiO$_2$ and Fe/TiO$_2$ catalysts prepared.

A color removal of 3 % was observed when iron-free TiO$_2$ was used as a catalyst. The presence of a small amount of iron could enhance the activity, but an excessive iron was unfavorable. This result can be attributed to the decrease of surface area of the catalyst with increasing iron content. A slight decrease in color (from 22.5 to 19.2 %) and COD (from 5 to 3 %) removal was observed after 2 h of reaction, while no significant change was obtained in initial degradation rate after 15 min of reaction time when iron content was increased from 1 to 5 wt%. The obtained color removal was much smaller than those given in the literature for the heterogeneous Fenton-like degradation of Rh6G in the presence of FeZSM-5 catalysts (Dükkancı et al. 2010a, b). In those studies after 2 h of reaction, a color removal of 98.7 % was obtained with an FeZSM-5 catalyst prepared by hydrothermal synthesis and a color removal of 27.6 % was achieved with an FeZSM-5 catalyst prepared by ion-exchange method.

The standard deviation of the average of independent runs changed in the range of ±0.97 to ±6.5 (Fig. 6a). The standard deviation for COD measurement was ±1.5. The rate constants were calculated and are given in Table 3.

UV light-assisted heterogeneous Fenton-like degradation of Rh6G

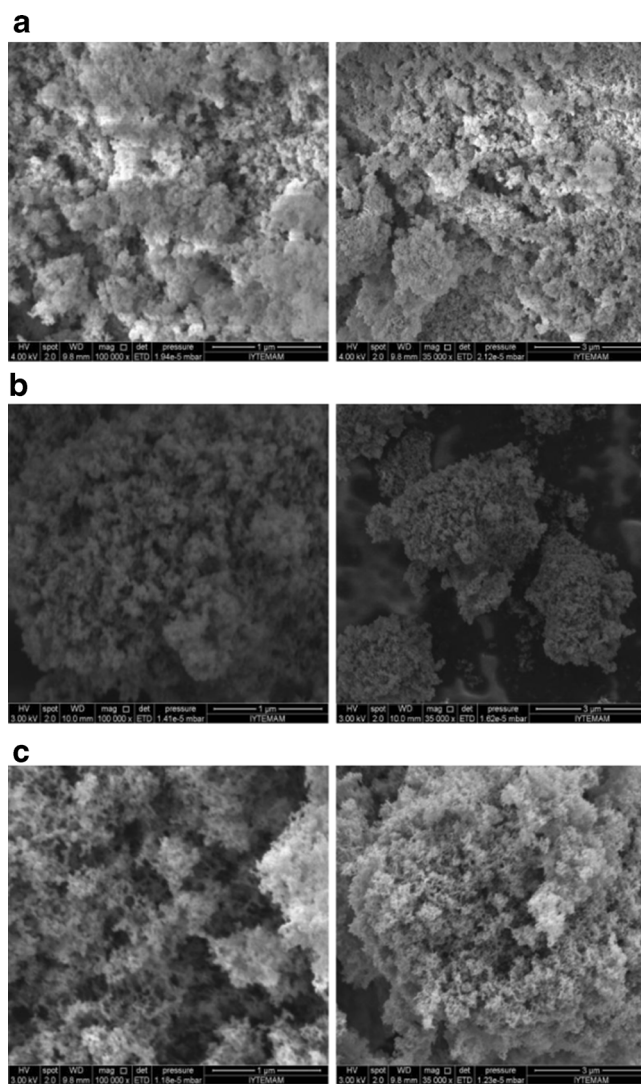Figure 7 displays the degradation of Rh6G with UV light-assisted heterogeneous Fenton-like process.

Table 2 The BET-surface area (S_{BET}), total pore volume (V_p), mean pore diameter (d_{mean}) and iron contents of the catalysts prepared

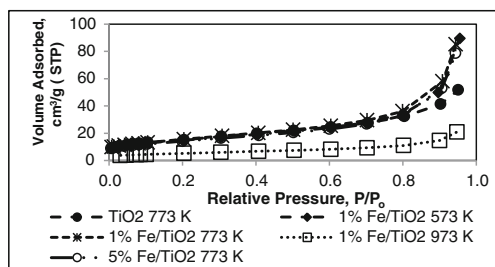| Catalysts	wt% Fe	S_{BET}, (m^2/g)	d_{mean}[a], nm	V_p, (cm^3/g)
TiO$_2$, 773 K	0	54.1	5.91	0.01400
1 % Fe/TiO$_2$, 573 K	0.93	52.2	10.02	0.01600
1 % Fe/TiO$_2$, 773 K	0.93	55.5	8.64	0.01500
1 % Fe/TiO$_2$, 973 K	0.93	18.6	6.89	0.00580
5 % Fe/TiO$_2$, 773 K	4.46	50.5	8.85	0.01388

[a] By BJH method

Fig. 5 Nitrogen adsorption isotherms of the samples

A drastic increase in color removal is achieved in degradation of Rh6G with the catalysts prepared in the presence of UV light. This result indicates that the prepared catalysts act as photocatalysts rather than Fenton catalysts. The highest initial degradation rate was obtained with 5 wt% Fe/TiO₂ catalyst. A color removal of 54 % was achieved after 15 min of reaction with this catalyst, and it showed the best decolorization until 60 min. Initial color removal increased with increasing iron content in the TiO₂ catalyst. However, color removal remained almost unchanged (>99 %) for iron-containing TiO₂ samples after 2 h of reaction. For this reason, from the point of saving the cost of iron, addition of iron in 1 wt% to TiO₂ seems to be sufficient to achieve complete color removal for Rh6G. Incorporation of 1 wt% of iron into TiO₂ affected positively the COD removal, while a slight decrease in COD removal was observed with 5 wt% Fe-containing TiO₂ catalyst. This catalyst has a lower surface area than 1 % Fe/TiO₂ catalyst. In the presence of TiO₂ (773 K) or 1 wt% Fe/TiO₂ (773 K) or 5 wt% Fe/TiO₂ (773 K) catalyst, the decolorization of Rh6G by the end of 60 min were 78.06, 91.48, and 95.09 %, respectively, in this study. However, Rh6G degraded by 50.8 % only in the presence of anatase TiO₂ nanoparticles under solar irradiation (Asiri et al. 2011) and by 7 % only in the presence of a template-free titania film (Elfeky and Al-Sherbini 2011).

The standard deviation of the average of independent runs changed in the range of ±0.01 to ±4.4 (Fig. 7a). The standard deviation for COD measurement was ±3.5. The rate constants were calculated and are given in Table 3.

Table 3 Rate constants calculated in Fenton-like oxidation (Fig. 6), UV assisted Fenton-like oxidation (Fig. 7), and sonophotoFenton oxidation (Fig. 8) runs of Rh6G

Catalysts	k, min⁻¹		
	Fenton	UV + Fenton	sonophotoFenton
TiO₂, 773 K	0.0008	0.0249	0.0878
1 % Fe/TiO₂, 773 K	0.0045	0.0291	0.1153
5 % Fe/TiO₂, 773 K	0.0062	0.0045	0.0980
1 % Fe/TiO₂, 573 K	n.m	0.0373	0.1088
1 % Fe/TiO₂, 973 K	n.m	0.0268	0.1064

n.m not measured

Degradation of Rh6G using sonophotoFenton process

When ultrasound (US) or UV light was applied alone for degradation of dye, a color removal of 3.5 and 6.1 % were achieved, respectively, after a reaction time of 90 min. In the combined use of ultrasound and UV light (sonophoto process without Fe/TiO₂ catalyst) for the oxidation of dye, a color removal of 15.2 % could be obtained after 90 min of reaction. COD removal was not observed.

In the ultrasound+UV light+H₂O₂-combined system, the effect of ultrasonic power was also investigated. In this concern, ultrasound+UV-light+H₂O₂ hybrid process was conducted at three different ultrasonic powers of 40, 80, and 100 W. As the power increased from 40 to 80 W and then to 100 W, there was almost no change in decolorization degree after a reaction time of 90 min. Whereas, increase in power decreased the COD reduction from 25 to 22 % and then to 18 %, respectively. So it could be said that 40-W ultrasonic power was sufficient.

SonophotoFenton oxidation runs of Rh6G took 1.5 h (excluding adsorption-desorption equilibrium) and were carried out at 293±2 K. Results are presented in Fig. 8.

Incorporation of iron into the TiO₂ did not change color removal after 1.5 h of reaction. However, initial color removal (after 15 min of reaction) increased from 72.3 to 80 % with addition of 1 wt% iron into the TiO₂, which was calcined at 573 K. A COD removal of 24 % was achieved with this
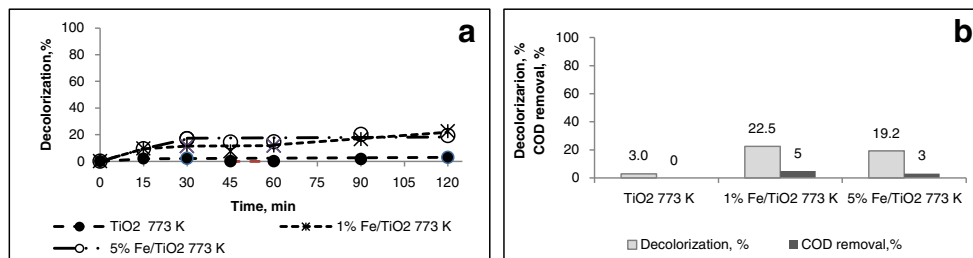

Fig. 6 The influence of catalyst type on degradation of Rh6G by heterogeneous Fenton-like process. **a** Decolorization %, **b** decolorization % and COD % removal after 2 h of reaction (*T*=323 K, initial concentration of Rh6G=20 ppm, H₂O₂ concentration=70 mM, catalyst amount=0.15 g/150 mL)
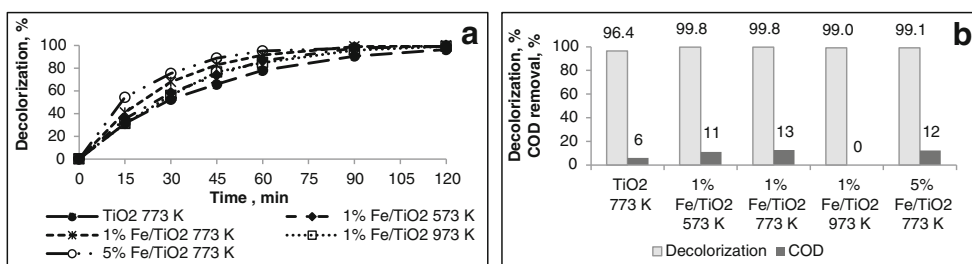
Fig. 7 The influence of catalyst type on degradation of Rh6G by UV assisted heterogeneous Fenton-like process. **a** Decolorization %, **b** decolorization % and COD % removal after 2 h of reaction (T=323 K, initial concentration of Rh6G=20 ppm, H_2O_2 concentration=70 mM, catalyst amount=0.15 g/150 mL, light sources=8 W UV-C lamp)

catalyst, while a COD removal of 14 % was obtained with iron-free TiO_2 catalyst. Initial color removal after 15 min and total COD abatement after 90 min decreased with increasing calcination temperature of the catalyst from 573 to 973 K. This result indicates that catalytic activity of the Fe/TiO_2 catalyst depends on the percentage of anatase phase in the TiO_2. As seen from Table 1, the percentage of anatase decreases from 81 % through 73.3 to 15.9 % with the increase of calcination temperature from 573 K through 773 to 973 K.

The better activity of the anatase TiO_2 may be due to the higher surface area and total pore volume. This plays an active role in the adsorption of dye, which results in its higher degradation. When these results are compared with the ones in the "UV light-assisted heterogeneous Fenton-like degradation of Rh6G" section, in which degradation of dye was achieved in the presence of UV light and Fenton process only, it is clearly seen that ultrasound has a positive contribution to COD removal and initial color removal after 15 min. COD removal increased from 13 % (reaction temperature=323 K, after 2 h) to 22 % (reaction temperature=293 K, after 1.5 h) in the presence of ultrasound when 1 wt% Fe/TiO_2 catalyst calcined at 773 K was used for oxidation.

The standard deviation of the average of independent runs changed in the range of ±0.01 to ±3.4 (Fig. 8a) and the standard deviation for COD measurement was ±0.5.

The rate constants were calculated and given in Table 3. Table 3 presents clearly the contribution of UV light to Fenton

oxidation and of ultrasound to photoFenton process. Rate constants in sonophotoFenton oxidation are much higher than those in Fenton and UV+Fenton processes. Rate constant in sonophotoFenton oxidation of Rh6G with 1 % Fe/TiO_2 calcined at 773 K is higher (0.1153 min^{-1}) than that with 1 % Fe/TiO_2 calcined at 573 K (0.1088 min^{-1}). However, color and COD removal are measured to be higher with the latter catalyst after a reaction time of 90 min (99.9 and 24 %, respectively, Fig. 8b). Consequently, the 1 % Fe/TiO_2 catalyst calcined at 573 K can be selected as an efficient catalyst in sonophotoFenton degradation of Rh6G under the operating conditions used in this study.

Adsorption of dye on Fe/TiO_2 catalysts was not higher than 1.5 % for all the runs done. During the runs, amount of iron loss into the solution was determined by measuring the iron concentration in the solution at the end of the reaction with atomic absorption spectrophotometer (varian-10 plus). Leached amount of iron was found to be less than 0.4 ppm for all the runs studied which was below the EU directives (<2 ppm).

Toxicity

L. Sativum L. (Garden cress) seeds were used to assess the toxicity of Rh6G solution prior to and after 90 min of sonophotoFenton treatment in the presence of 1 % Fe/TiO_2 catalyst, which was calcined at 573 K. In the procedure, 5 ml
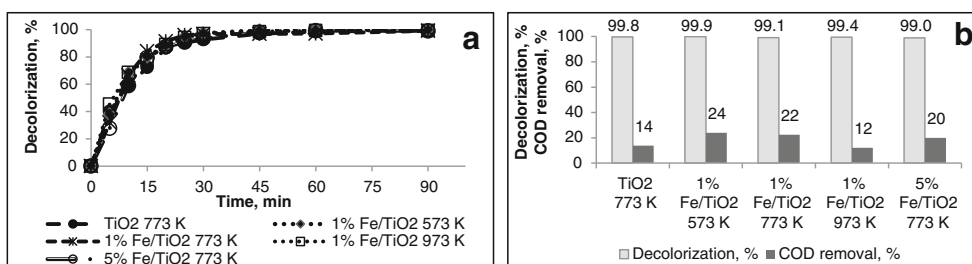

Fig. 8 The influence of catalyst type on degradation of Rh6G by sonophotoFenton process. **a** Decolorization, %, **b** decolorization % and COD % removal after 90 min of reaction (T=293 K, initial concentration of Rh6G=20 ppm, H_2O_2 concentration=70 mM, catalyst amount= 0.325 g/650 mL, light sources=4 W+4 W UV-C lamp, ultrasonic power=40 W, 20 kHz)

of treated and untreated Rhodamine 6G solution (20 ppm) and pure water were pipetted onto a filter paper fitted into a 9-cm glass Petri dish. Then 25 seeds of cress were distributed evenly on them. These three Petri dishes were placed in the dark for 72 h, after that time, root lengths of seeds were measured for pure water, treated and untreated wastewaters. Inhibition % value was calculated according to equation given below for treated and untreated wastewater:

$$\text{Inhibition}, \% = \frac{\text{Root Length}_{\text{pure water}} - \text{Root Length}_{\text{sample}}}{\text{Root Length}_{\text{pure water}}} \quad (3)$$

Inhibition, % values are 75 and 15 % for untreated and treated Rhodamine 6G solutions, respectively. The descend in the inhibition value shows that it could be achieved to decrease toxicity of the Rhodamine 6G under the experimental conditions used (Devare and Bahadır 1994; Arambasic et al. 1995; Alkan et al. 2006; Terzi 2008).

Conclusion

This study showed that the combination of ultrasound and UV with heterogeneous Fenton process is efficient for the complete color removal of Rh6G. The 1 wt% iron-containing TiO_2 catalyst calcined at 573 K behaves as efficient and stable catalyst for the integrated heterogeneous sonophotoFenton degradation of Rh6G. The catalytic activity of the catalyst depends on the percentage of anatase phase in the TiO_2. At the experimental conditions of 650 mL of 20 ppm Rh6G solution, 70 mM H_2O_2, 0.325 g of catalyst, 293±2 K reaction temperature, an ultrasonic power of 40 W at 20 kHz, UV-C lamp at 4 W+4 W, a color removal of 99.9 %, and a COD removal of 24 % could be achieved after 90 min of reaction.

Consequently, the heterogeneous sonophotoFenton system appears as a promising process for Rh6G wastewater treatment.

References

Aarthi T, Madras G (2007) Photocatalytic degradation of Rhodamine dyes with Nano-TiO_2. Ind Eng Chem Res 46:7–14

Akpan UG, Hameed BH (2009) Parameters affecting the photocatalytic degradation of dyes using TiO_2-Based photocatalysts: a review. J Hazard Mater 170:520–529

Alkan U, Çalışkan-Eleren S, Odabaş E (2006) Cr^{+6} ve Zn^{+2} metallerinin aktif çamur sistemine toksik etkileri. Uludağ Üniversitesi Mühendislik-Mimarlık Fakültesi Dergisi 11:93–102

Arambasic MB, Bjelic S, Subakov G (1995) Acute toxicity of heavy metals (copper, lead, zinc), phenol and sodium on *Allium Cepa* L., *Lepedium Stavum* L. and *Daphnia Magna* St.: comparative investigations and the practical applications. Water Res 29:497–503

Arana J, Diaz G, Saracho MM, Rodriguez JMD, Melian JAH, Pena JP (2002) Maleic acid photocatalytic degradation using Fe-TiO_2 catalysts dependence of the degradation mechanism on the Fe catalysts content. Appl Catal B Environ 36:113–124

Arana J, Gonzalez Diaz O, Dona Rodriguez JM, Herrera Melian JA, Garrigai Cabo C, Perez Pena J, Carmen Hidalgo M, Navio-Santos JA (2003) Role of Fe^{3+}/Fe^{2+} as TiO_2 dopant ions in photocatalytic degradation of carboxylic acids. J Mol Catal A Chem 197:157–171

Asiri AM, Al-Amoudi MS, Al-Talhi TA, Al-Talhi AD (2011) Photo degradation of Rhodamine 6G and phenol red by nanosized TiO_2 under solar irradiation. J Saudi Chem Soc 15:121–128

Berberidou C, Poulios I, Xekoukoulotakis NP, Mantzavinos D (2007) Sonolytic, photocatalytic and sonophotocatalytic degradation of malachite green in aqueous solutions. Appl Catal B Environ 74:63–72

Beyers E, Biermans E, Ribbens S, De Witte K, Mertens M, Meynen V, Bals S, Van Tendeloo G, Vansat EF, Lool P (2009) Combined TiO_2/SiO_2 mesoporous photocatalysts with location and phase controllable TiO_2 nano particles. Appl Catal B Environ 88:515–524

Bouras P, Lianos P (2008) Synergy effect in the combined photodegradation of an azo dye by titanium dioxide photocatalysis and photo-Fenton oxidation. Catal Lett 123:220–225

Buddee S, Wongnawa S, Sirimahachai U, Puetpaibool W (2011) Recyclable UV and visible light photocatalytically active amorphous TiO(2) doped with M (III) ions (M = Cr and Fe). Mater Chem Phys 126:167–177

Chen J, Liu M, Zhang L, Zhang J, Jin L (2003) Application of nano TiO_2 towards polluted water treatment combined with electrophotochemical method. Water Res 37:3815–3820

De Witte K, Busuioc AM, Meynen V, Mertens M, Bilba N, Van Tendeloo G, Cool P, Vansant EF (2008) Influence of the synthesis parameters of TiO_2-SBA-15 materials on the adsorption and photodegradation of rhodamine-6G. Microporous Mesoporous Mater 110:100–110

Devare M, Bahadır M (1994) Biological monitoring of Landfill leachate using plants and luminescent bacteria. Chemosphere 28:261–271

Dükkancı M, Gündüz G, Yılmaz S, Yaman YC, Prikhodko RV, Stolyarova IV (2010a) Characterization and catalytic activity of CuFeZSM-5 catalysts for oxidative degradation of Rhodamine 6G in aqueous solutions. Appl Catal B Environ 95:270–278

Dükkancı M, Gündüz G, Yılmaz S, Prihodko RV (2010b) Heterogeneous Fenton-like degradation of Rhodamine 6G in water using CuFeZSM-5 zeolite catalyst prepared by hydrothermal synthesis. J Hazard Mater 181:343–350

Dutta K, Mukhapadhyay S, Bhattacharjee S, Chaudhuri B (2001) Chemical oxidation of methylene blue using a Fenton-like reaction. J Hazard Mater B84:57–71

Elfeky SA, Al-Sherbini AA (2011) Photo-oxidation of Rhodamine 6G via TiO_2 and Au/TiO_2-bound polythene beads. J Nano Mater 74:1–8

Feng JY, Wong RSK, Hu XJ, Yue PL (2004) Discoloration and mineralization of orange II by using Fe^{3+}-doped TiO_2 and bentonite clay-based Fe nanocatalysts. Catal Today 98:441–446

Ghazzal MN, Kebaili H, Joseph M, Debecker DP, Elay P, De Coninck J, Gaigneaux EM (2012) Photocatalytic degradation of Rhodamine 6G on mesoporous titania films. Appl Catal B Environ 115–116:276–284

Hafizah N, Sopyan I (2009) Nanosized TiO_2 photocatalyst powder via sol-gelmethod: effect of hydrolysis degree on powder properties. Int J Photoenergy Article ID 962783, 8 pages doi:10.1155/2009/962783

He ZQ, Song S, Xia M, Qiu JP, Ying HP, Lu BS, Jiang YF, Chen JM (2007) Mineralization of CI reactive yellow 84 in aqueous solution by sonolytic ozonation. Chemosphere 69:191–199

Hossenia A, Keyanpour-Rad M, Pazouki M (2010) Photo-catalytic degradation of organic dyes with different chromophores by synthesized nanosize TiO$_2$ particles. World Appl Sci J 8:1327–1332

İnce HN, Tezcanlı G (2001) Reactive dyestuff degradation by combined sonolysis and ozonation. Dyes Pigments 49:145–153

Jamalluddin NA, Abdullah AZ (2011) Reactive dye degradation by combined Fe(III)/TiO$_2$ catalyst and ultrasonic irradiation: effect of Fe (III) loading and calcination temperature. Ultrason Sonochem 18:669–678

Jiang Y, Petrier C, Waite TD (2002) Effect of pH on the ultrasonic degradation of ionic aromatic compounds in aqueous solution. Ultrason Sonochem 9:163–168

Jiefang Z, Qiaorong S, Wei Z, Bin H, Jinlong Z, Anpo M (2003) Characterization and photocatalytic reactivity of Fe/TiO2 photocatalysts synthesized by hydrothermal method, www.paper.edu.cn/download/downPaper/200312-45

Kansal SK, Singh M, Sud D (2007) Studies on pohotodegradation of two commercial dyes in aqueous phase using different photocatalysts. J Hazard Mater 141:581–590

Khalid NR, Ahmed E, Ikram M, Ahmed M, Phoenix DA, Elhissi A, Ahmed W, Jackson MS (2013) Effects of calcination on structural photocatalytic properties of TiO$_2$ nanopowders via TiCl$_4$ hydrolysis. J Mater Eng Perform 22:371–375

Konstantinou IK, Albanis TA (2004) TiO$_2$-assisted photocatalytic degradation of azo dyes in aqueous solution: kinetic and mechanistic investigations: a review. Appl Catal B Environ 49:1–14

Kusic H, Koprivanac N, Srsan L (2006) Azo dye degradation using Fenton type processes assisted by UV irradiation: a kinetic study. J Photochem Photobiol A Chem 181:195–202

Liu Y, Sun DZ, Cheng L, Li YP (2006) Preparation and characterization of Fe$_2$O$_3$-CeO$_2$-TiO$_2$/gamma-Al$_2$O$_3$ catalyst for degradation dye wastewater. J Environ Sci China 18:1189–1192

Meng NG, Chen P-C, Manickam S (2012) Hydrothermal crystallization of titania on silver nucleation sites for the synthesis of visible light nano-photocatalysts—enhanced photoactivity using Rhodamine 6G. Appl Catal A Gen 433–434:75–80

Mi JL, Johnsen S, Clausen C, Hald P, Lock N, Sø L, Iversen BB (2013) Highly controlled crystallite size and crystallinity of pure and iron-doped anatase-TiO$_2$ nanocrystals by continuous flow supercritical synthesis. J Mater Res 28:333–339

Nam SN, Han SK, Kang JW, Choi H (2003) Kinetics and mechanisms of the sonolytic destruction of non-volatile organic compounds: investigation of the sonochemical reaction zone using several OH$^.$ monitoring techniques. Ultrason Sonochem 10:139–147

Neamtu M, Yediler A, Siminiceanu I, Kettrup A (2003) Oxidation of commercial reactive azo dye aqueous solutions by the photo-Fenton and Fenton-like processes. J Photochem Photobiol A Chem 161:87–93

Neamtu M, Yediler A, Siminiceanu I, Macoveanu M, Kettrup A (2008) Photodegradation of reactive yellow 84 azo-dye in aqueous solution. Toxicol Environ Chem 78:31–40

Okuno H, Yim B, Mizukoshi Y, Nagata Y, Maeda Y (2000) Sonolytic degradation of hazardous organic compounds in aqueous solution. Ultrason Sonochem 7:261–264

Prihodko R, Stolyarova I, Gündüz G, Taran O, Yashnik S, Parmon V, Goncharuk V (2011) Fe-exchanged zeolites as materials for catalytic wet peroxide oxidation. Degradation of Rodamine G dye. Appl Catal B Environ 104:201–210

Rehopek A, Tauber M, Gübitz G (2004) Application of power ultrasound for azo dye degradation. Ultrason Sonochem 11:177–182

Sivakumar M, Tatake PA, Pandit AB (2002) Kinetics of p-nitrophenol degradation: effect of reaction conditions and cavitational parameters for a multiple frequency system. Chem Eng J 85:327–338

Souza MCP, Lenzi GG, Colpini LMS, Jorge LMM, Santos OAA (2011) Photocatalytic discoloration of reactive blue 5G dye in the presence of mixed oxides and with the addition of iron and silver. Braz J Chem Eng 28:393–402

Stasinakis AS (2008) Use of selected advanced oxidation processes (AOPs) for wastewater treatment—a mini review. Glob NEST J 10:376–385

Sun S, Ding J, Bao J, Gao C, Zeming Q, Yang X, He B, Li C (2012) Photocatalytic degradation of gaseous toluene on Fe-TiO$_2$ under visible light irradiation: a study on the structure, activity and deactivation mechanism. Appl Surf Sci 58:5031–5037

Tayade RJ, Surolia PK, Kulkarni RG, Jasra RV (2007) Photocatalytic degradation of dyes and organic contaminants in water using nanocrystalline anatase and rutile TiO$_2$. Sci Technol Adv Mater 8:455–462

Terzi I (2008) Allelopathic effects of Juglone and decomposed walnut leaf juice on muskmelon and cucumber seed germination and seedling growth. Afr J Biotechnol 7:1870–1874

Tezcanli-Güyer G, İnce NH (2004) Individual and combined effects of ultrasound, ozone and UV irradiation: a case study with textile dyes. Ultrasonics 42:603–609

Tezcanlı-Güyer G, İnce NH (2003) Degradation and toxicity reduction of textile dyestuff by ultrasound. Ultrason Sonochem 10:235–240

Torrades F, Garcia-Montano J, Garcia-Hortal JA, Nunez L, Domenech X, Peral J (2004) Decolorization and mineralization of homo- and hetero-bireactive dyes under Fenton and photo-Fenton conditions. Colororation Technol 120:188–194

Wang XK, Chen GH, Guo WL (2003) Sonochemical degradation kinetics of methyl violet in aqueous solutions. Molecules 8:40–44

Wang AJ, Cuan A, Salmones J, Nava N, Castillo S, Moran-Pineda M, Rojas F (2004) Studies of sol-gel TiO$_2$ and Pt/TiO2 catalysts for NO reduction by CO in an oxygen reach condition. Appl Surf Sci 230:94–105

Zhao BX, Shi BC, Zhang XL, Cao X, Zhang YZ (2011) Catalytic wet hydrogen peroxide oxidation of H-acid in aqueous solution with TiO($_2$)-CeO($_2$) and Fe/TiO($_2$)-CeO($_2$) catalysts. Desalination 268:55–59

Zhong X, Royer S, Zhang H, Huang Q, Xiang L, Valange S, Barrault J (2011) Mesoporous silica Iron-doped as stable and efficient heterogeneous catalyst for the degradation of C.I. Acid Orange 7 using sono–photo-Fenton process. Sep Purif Technol 80:163–171